Joint Spectrum Leasing and Power Allocation Optimization of Virtual Mobile Network

Miao Jiang, Yiqing Li, Qi Zhang, *Member*, *IEEE*, and Jiayin Qin

***Abstract*—**

***Index Terms*—Unmanned aerial vehicle (UAV), wireless powered communication network, sequential unconstrained convex minimization, Dinkelbach.**

I. INTRODUCTION

To satisfy dramatic traffic growth over the next decade, 5G mobile networks are expected to achieve higher data rates, enhanced end-user quality-of-service (QoS) and reduced transmission latency [1], [2]. Wireless network virtualization (WNV) is a promising solution to satisfy the rapid development of 5G [3]. WNV can facilitate multiple network operators to share common resources, e.g., licensed spectrum. The virtualized wireless networks consist of MNO (mobile network operator) and MVNO (mobile virtual network operator) [4]. The MNO owns the physical cellular infrastructure and radio resources, it executes the virtualization by leasing the isolated virtualized network resources to the MVNO. The MVNO leases the resources from the MNO and then assigns the resources to the MUs (mobile users). The spectrum resources belong to one or more MNOs and are virtualized and spitted into slices. The MVNO utilizes the slices from MNOs depending on the QoS of MUs.

In recent years, WNV has attracted an increasing attention in standardization bodies, industrial societies and academia [5]–[11].

QoS survey the alternating direction method of multipliers (ADMM)

distributed optimization scheme

II. SYSTEM MODEL AND PROBLEM FORMULATION

Consider a wireless communication system with one MNO and N MVNOs. With wireless network virtualization operation, the whole communication processes are divided into two stages. MVNOs will first rent wireless spectrum from the MNO and then provide customized services to their MUs in respective service cell. Particularly, we investigate a OFDMA (orthogonal frequency division multiple access)

downlink transmission scenario, where the total bandwidth owned by MNO is W_{sum} Hertz (Hz).

During the first transmission stage, the bandwidth occupied by the i-th MVNO is denoted as w_i. Thus, we have

$$\sum_{i=0}^{N} w_i \leq W_{sum}. \qquad (1)$$

In this paper, without loss of generality, we assume that the i-th MVNO is located as the origin o_i. The locations of MUs are modeled as a realization of a Poisson point process (PPP) with intensity λ_i in a fixed circular region $\mathcal{D}(o_i, r_i) \in \mathbb{R}^2$, where r_i denotes the cell radius. The locations of MUs associated with the i-th MVNO are denoted as $\mathcal{X} = \{\mathbf{x}_{ij} \in \mathbb{R}^2 | j = 1, \cdots, N_i\}$, where $N_i = \pi r_i^2 \lambda_i$ is the expected number of MUs in the i-th MVNO. Note that the user set $\mathcal{X}$ changes with user arrivals, departure, or movements.

Suppose that transmitted signals are affected by both large-scale path loss and fast Rayleigh fading. Thus, the channel between the j-th MU and its associated i-th MVNO is denoted by $h_{ij} = \frac{g_{ij}}{\sqrt{1+\|\mathbf{x}_{ij}\|^\alpha}}$, where α denotes the path-loss decay factor and g_{ij} denotes the Rayleigh fading channel state information (CSI), i.e., g_{ij} is a complex Gaussian random variable with zero mean and unit variance. The instantaneous data rate for the j-th MU in the i-th MVNO is given by

$$R_{ij} = b_{ij} \log_2 \left(1 + \frac{q_{ij} |h_{ij}|^2}{\Gamma b_{ij} n_0}\right) \qquad (2)$$

where b_{ij} denotes the bandwidth of the j-th MU allocated by the i-th MVNO, q_{ij} denotes the power allocated to the j-th MU by the i-th MVNO. Γ denotes the SNR gap to the information theoretical channel capacity owing to the non-ideal coding and modulation in practice [12]. n_0 denotes the power spectral density of white noise at the MU.

The two-stage spectrum leasing processes are operated in two timescales, namely a period and a time slot. As shown in Fig. 1, the first stage is operated in a period and often measured in hours, where each MVNO rents wireless spectrum from a MNO. The second stage is operated in a time slot and often measured in milliseconds, during which the wireless channel fading remains constant but may change from one time slot to anther. Notice that MVNOs will not release the occupied spectrum until the end of the whole transmission. We will discuss these two stages in the following two sections.
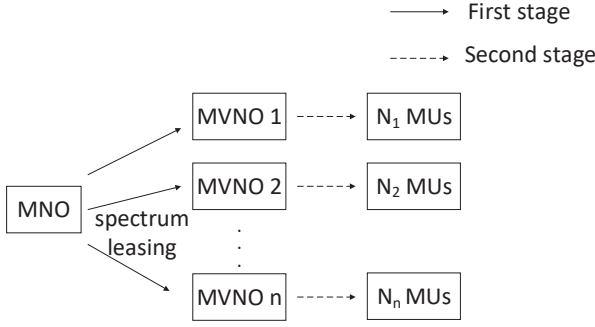
Fig. 1. Two-stage spectrum leasing network. During the first stage, MVNOs rent spectrum from an MNO based on the arrival rate and QoS of MUs. During the second stage, each MVNO allocates the obtained spectrum dynamically to a set of MUs.

III. SPECTRUM LEASING AND POWER ALLOCATION DURING THE FIRST STAGE

A. Problem formulation

During the first stage, the CSI of each MU in each MVNO is a random variable. So, we first assume that the bandwidth and power allocated to all MUs in each MVNO are equal. Thus, the expected data rate of the j-th MU in the i-th MVNO is expressed as

$$E\left(R_{ij}\right) = \int_0^\infty \frac{w_i}{n_i} \log_2\left(1 + \frac{p_i x}{w_i n_0}\right) f_{|h_{ij}|^2}(x)\, dx \quad (3)$$

where P_i denotes the total transmission power budget for the i-th MVNO, $f_{|h_{ij}|^2}(x)$ is the probability density function (PDF) of the random variable $|h_{ij}|^2$.

During the first stage, we aim at minimizing the total transmit power at MVNOs under the QoS requirement at each MU in each MVNO and the total bandwidth constraint at the MNO by properly choosing the transmit power p_i and the bandwidth w_i. Thus, the optimization problem is formulated as

$$\min_{\mathbf{p},\mathbf{w}} \sum_{i=1}^N p_i \quad (4a)$$

$$\text{s.t.} \quad \sum_{i=1}^N w_i \leq W_{sum} \quad (4b)$$

$$E\left(R_{ij}\right) \geq \bar{R}_i,\ p_i \geq 0, w_i \geq 0,\ \forall i, \quad (4c)$$

where $\bar{R}_i$ denotes the data rate threshold at the i-th MVNO [1], $\mathbf{p} = [p_1, p_2, \cdots, p_N]^T$, $\mathbf{w} = [w_1, w_2, \cdots, w_N]^T$. To proceed, we will first introduce the following proposition:

Proposition 1: The cumulative distribution function (CDF) of $|h_{ij}|^2$ is $F_{|h_{ij}|^2}(x) = 1 - M\left(\frac{2}{\alpha}, 1 + \frac{2}{\alpha}, -xr_i^\alpha\right) e^{-x}$, where $M(a, b, z)$ denotes the Kummer's function [13].

[1]Note that in this paper, we assume that the data rate thresholds at different MUs which associated with the same MVNO are equal due to the same distribution of different MUs in each MVNO.

Proof: See Appendix A. ∎

Using the above proposition 1, $f_{|h_{ij}|^2}(x)$ can be calculated as follows:

$$f_{|h_{ij}|^2}(x)$$
$$= \frac{dF_{|h|_{ij}^2}(x)}{dx}$$
$$= M\left(\frac{2}{\alpha}, 1 + \frac{2}{\alpha}, -xr_i^\alpha\right) e^{-x} - \frac{dM\left(\frac{2}{\alpha}, 1 + \frac{2}{\alpha}, -xr_i^\alpha\right)}{dx} e^{-x}$$
$$\overset{(d)}{=} M\left(\frac{2}{\alpha}, 1 + \frac{2}{\alpha}, -xr_i^\alpha\right) e^{-x} +$$
$$\frac{2}{2+\alpha} M\left(1 + \frac{2}{\alpha}, 2 + \frac{2}{\alpha}, -xr_i^\alpha\right) r_i^\alpha e^{-x}$$
$$= e^{-x} g(x) \quad (5)$$

where (d) follows from $\frac{dM(a,b,z)}{dz} = \frac{a}{b} M(a+1, b+1, z)$ [13, 13.4.8], $g(x)$ is defined as follows:

$$g(x) = \frac{2r_i^\alpha}{2+\alpha} M\left(1 + \frac{2}{\alpha}, 2 + \frac{2}{\alpha}, -xr_i^\alpha\right) +$$
$$M\left(\frac{2}{\alpha}, 1 + \frac{2}{\alpha}, -xr_i^\alpha\right). \quad (6)$$

Now, the original optimization problem (4) can be reformulated as follows:

$$\min_{\mathbf{p},\mathbf{w}} \sum_{i=1}^N p_i \quad (7a)$$

$$\text{s.t.} \quad \sum_{i=1}^N w_i \leq W_{sum} \quad (7b)$$

$$\int_0^\infty \frac{w_i}{n_i} \log_2\left(1 + \frac{p_i x}{w_i n_0}\right) e^{-x} g(x)\, dx \geq \bar{R}_i, \forall i \quad (7c)$$

$$p_i \geq 0, w_i \geq 0,\ \forall i, \quad (7d)$$

it is observed in (7c), the calculation of the integration is complicated and can be calculated via numerical integration. Denote the left-hand sides (LHSs) of (7c) as $q(p_i, w_i)$. The numerical integration can be very time-consuming when the integrand of $\kappa(p_i, w_i)$ has a heavy tail. Thus, next we will apply half-range Gauss-Hermite Quadrature (HR-GHQ) to approximate $q(p_i, w_i)$ with high accuracy [14], [15].

Based on [15], a K-point HR-GHQ can be written as

$$\int_0^\infty e^{-x^2} f(x)\, dx \approx \sum_{k=1}^K a_k f(x_k) \quad (8)$$

where both the weights $\{a_k\}_{k=1}^K$ and abscissas $\{x_k\}_{k=1}^K$ are real numbers. After applying (8) to $\kappa(p_i, w_i)$, we have

$$\kappa(p_i, w_i) \overset{(e)}{=} \int_0^\infty e^{-t^2} \frac{w_i}{n_i} g\left(t^2\right) 2t \log_2\left(1 + \frac{p_i t^2}{w_i n_0}\right) dt$$
$$\overset{(f)}{\approx} \sum_{i=1}^{K_i} a_{ki} \frac{w_i}{n_i} g\left(t_{ki}^2\right) 2t_{ki} \log_2\left(1 + \frac{p_i t_{ki}^2}{w_i n_0}\right)$$
$$\overset{(g)}{=} \sum_{k=1}^{K_i} b_{ki} \frac{w_i}{n_i} \log_2\left(1 + \frac{p_i t_{ki}^2}{w_i n_0}\right) \quad (9)$$

where (e) follows from $x = t^2$, (f) follows from (8), (g) follows from $b_{ki} = a_{ki}g\left(t_{ki}^2\right)2t_{ki}$.

Finally, the spectrum leasing allocation optimization problem can be expressed as follows:

$$\min_{\mathbf{p},\mathbf{w}} \sum_{i=1}^{N} p_i \tag{10a}$$

$$\text{s.t.} \quad \sum_{i=1}^{N} w_i \leq W_{sum} \tag{10b}$$

$$\sum_{k=1}^{K_i} b_{ki}\frac{w_i}{n_i}\log_2\left(1 + \frac{p_i t_{ki}^2}{w_i n_0}\right) \geq \bar{R}_i, \forall i \tag{10c}$$

$$p_i \geq 0, w_i \geq 0, \ \forall i. \tag{10d}$$

Since problem (10) is convex in terms of optimization variables $\mathbf{p}$ and $\mathbf{w}$, it can be solved efficiently by existing optimization tools such as CVX [16]. Next, we will exploit the structure of problem (10) and obtain its global optimal solution via using a distributed algorithm named ADMM [17], [18] to further reduce the complexity.

B. ADMM-based distributed algorithm for solving optimization problem (10)

First, we will introduce an auxiliary variable $\mathbf{z} = [z_1, z_2, \cdots, z_N]^T$. Thus, optimization problem (10) can be reformulated as

$$\min_{\mathbf{p},\mathbf{w},\mathbf{z}} \sum_{i=1}^{N} p_i \tag{11a}$$

$$\text{s.t.} \quad \mathbf{w} - \mathbf{z} = \mathbf{0} \tag{11b}$$

$$\sum_{i=1}^{N} z_i \leq W_{sum} \tag{11c}$$

$$\sum_{k=1}^{K_i} b_{ki}\frac{w_i}{n_i}\log_2\left(1 + \frac{p_i t_{ki}^2}{w_i n_0}\right) \geq \bar{R}_i, \forall i \tag{11d}$$

$$p_i \geq 0, w_i \geq 0, z_i \geq 0, \ \forall i. \tag{11e}$$

Denote the feasible region of constraint (11c) and $z_i \geq 0, \forall i$ as $\mathcal{C}$, its indicator function can be defined as

$$\mathbb{I}_{\mathcal{C}}(\mathbf{z}) = \begin{cases} 0, & \text{if } \mathbf{z} \in \mathcal{C}, \\ +\infty, & \text{otherwise.} \end{cases} \tag{12}$$

Likewise, denote the feasible region of constraint (11d), $p_i \geq 0$ and $w_i \geq 0, \forall i$ as $\mathcal{D}$, its indicator function can be defined as

$$\mathbb{I}_{\mathcal{D}}(\mathbf{p},\mathbf{w}) = \begin{cases} 0, & \text{if } (\mathbf{p},\mathbf{w}) \in \mathcal{D}, \\ +\infty, & \text{otherwise.} \end{cases} \tag{13}$$

Thus, problem (11) can be rewritten in ADMM form as follows:

$$\min_{\mathbf{p},\mathbf{w},\mathbf{z}} \sum_{i=1}^{N} p_i + \mathbb{I}_{\mathcal{C}}(\mathbf{z}) + \mathbb{I}_{\mathcal{D}}(\mathbf{p},\mathbf{w}) \tag{14a}$$

$$\text{s.t.} \quad \mathbf{w} - \mathbf{z} = \mathbf{0} \tag{14b}$$

Then, the augmented Lagrangian (using the scaled dual variable) of problem (14) is given by

$$\mathcal{L}_{\rho}(\mathbf{p},\mathbf{w},\mathbf{z},\mathbf{u}) = \sum_{i=1}^{N} p_i + \mathbb{I}_{\mathcal{C}}(\mathbf{z}) + \mathbb{I}_{\mathcal{D}}(\mathbf{p},\mathbf{w}) +$$
$$\frac{\rho}{2}\|\mathbf{w} - \mathbf{z} + \mathbf{u}\|_2^2 \tag{15}$$

where $\rho > 0$ is the penalty parameter and $\mathbf{u} = [u_1, u_2, \cdots, u_N]^T$ is the dual variable for the constraint (??). From problem (14), it can be observed that the variables can be split into two blocks: $\{\mathbf{p}, \mathbf{w}\}$ and $\mathbf{z}$. Besides, the objective function is also separable across this splitting. Therefore, the ADMM technique can be applied to solve this problem by iteratively updating $\{\mathbf{p}, \mathbf{w}\}$, $\mathbf{z}$ and $\mathbf{u}$. Denote the values in the k-th iteration as $\{\mathbf{p}^k, \mathbf{w}^k, \mathbf{z}^k, \mathbf{u}^k\}$. Thus, in the $(k+1)$-th iteration, the variables can be updated sequentially as follows:

1) step 1: Given $\{\mathbf{z}^k, \mathbf{u}^k\}$, we first maximize $\mathcal{L}_{\rho}$ with respect to $\{\mathbf{p}, \mathbf{w}\}$, where

$$\{\mathbf{p}^{k+1}, \mathbf{w}^{k+1}\} = \arg\max_{\mathbf{p},\mathbf{w}} \mathcal{L}_{\rho}(\mathbf{p},\mathbf{w},\mathbf{z}^k,\mathbf{u}^k) \tag{16}$$

Notice that the update of $\mathbf{p}$ and $\mathbf{w}$ in problem (16) is equivalent to solving the following problem:

$$\min_{\mathbf{p},\mathbf{w}} \sum_{i=1}^{N} p_i + \frac{\rho}{2}\sum_{i=1}^{N}\left(w_i - z_i^k + u_i^k\right)^2 \tag{17a}$$

$$\text{s.t.} \quad \text{(11d)}, \tag{17b}$$

$$w_i \geq 0, p_i \geq 0, \forall i. \tag{17c}$$

It is observed that problem (17) can be decomposed into N subproblems, each subproblem solves:

$$\min_{p_i,w_i} p_i + \frac{\rho}{2}\left(w_i - z_i^k + u_i^k\right)^2 \tag{18a}$$

$$\text{s.t.} \quad \sum_{k=1}^{K_i} b_{ki}\frac{w_i}{n_i}\log_2\left(1 + \frac{p_i t_{ki}^2}{w_i n_0}\right) \geq \bar{R}_i, \tag{18b}$$

$$w_i \geq 0, p_i \geq 0. \tag{18c}$$

Notice that each subproblem (18) is a convex problem and can be solved efficiently using interior point method [19].

2) step 2: Given $\{\mathbf{p}^{k+1}, \mathbf{w}^{k+1}, \mathbf{u}^k\}$, we then maximize $\mathcal{L}_{\rho}$ with respect to $\mathbf{z}$, where

$$\mathbf{z} = \arg\max_{\mathbf{z}} \mathcal{L}_{\rho}(\mathbf{p}^{k+1},\mathbf{w}^{k+1},\mathbf{z},\mathbf{u}^k), \tag{19}$$

which can be equivalently written as the following convex optimization problem:

$$\min_{\mathbf{z}} \|\mathbf{w}^{k+1} - \mathbf{z} + \mathbf{u}^k\|_2^2 \tag{20a}$$

$$\text{s.t.} \quad \|\mathbf{z}\|_1 \leq W_{sum}, \tag{20b}$$

$$z_i \geq 0, \forall i. \tag{20c}$$

The above convex problem (20) is the l_1 ball problem [20] and we can obtain its closed-form solution as follows:

(a) If $\|\mathbf{w}^{k+1} + \mathbf{u}^k\|_1 > W_{sum}$, z_i^{k+1} can be obtained as follows:

$$z_i^{k+1} = \max\{w_i^{k+1} + u_i^k - \beta, 0\} \tag{21}$$

where $\beta = \frac{1}{\zeta}\left(\sum_{i=1}^{\zeta} v_i - W_{sum}\right)$, $\mathbf{v} = [v_1, v_2, \cdots, v_N]^T$ and $\mathbf{v}$ denotes the vector obtained by sorting $\mathbf{w}^{k+1} + \mathbf{u}^k$ in a descending order. ζ is denoted as

$$\zeta = \max_{1 \leq i \leq N}\left\{ i \left| v_i - \frac{1}{i}\left(\sum_{j=1}^{i} v_j - W_{sum}\right) > 0 \right.\right\} \quad (22)$$

(b) If $\left\|\mathbf{w}^{k+1} + \mathbf{u}^k\right\|_1 \leq W_{sum}$, z_i^{k+1} can be obtained as

$$z_i^{k+1} = w_i^{k+1} + u_i^k \quad (23)$$

3) step 3: Given $\{\mathbf{w}^{k+1}, \mathbf{z}^{k+1}\}$, we minimize $\mathcal{L}_\rho$ with respect to $\mathbf{u}$, which is achieved by updating the dual variable $\mathbf{u}$ as

$$\mathbf{u}^{k+1} = \mathbf{w}^{k+1} - \mathbf{z}^{k+1} + \mathbf{u}^k \quad (24)$$

1: **Initialize:** $w_i^0 = \frac{W_{sum}}{N_i}$, p_i^0, $z_i^0 = 0$, and $u_i^0 = 0$, $\forall i$. $k = 0$. Set the penalty parameter $\rho = 1$.
2: **Repeat:**
 Each MVNO updates its local variables $\{w_i^{k+1}, p_i^{k+1}\}$ by solving (18) in parallel and the obtained results $\{w_i^{k+1}\}$ are passed to the MNO;
 The MNO updates the variable $\mathbf{z}^{k+1}$ with closed-form expression (21);
 The MNO updates the dual variable $\mathbf{u}^{k+1}$ using (24);
 $k := k + 1$;
3: **Until:** convergence.

Algorithm 1: The proposed ADMM based method for solving problem (10).

---

initialize: Set $z_i^0 = 0$ and $u_i^0 = 0$, $\forall i$ on blockchain, $k = 0$.
repeat
 P_i: *Optimization for each MVNO, compute locally*
  Get z_i^k and u_i^k from blockchain;
  Update w_i^{k+1} and p_i^{k+1} by solving (18);
  Send w_i^{k+1} to smart contract S_0;
 S_0: *ADMM aggregator, compute on blockchain*
  Update $\mathbf{z}^{k+1}$ with closed-form expression (21);
  Update the dual variable $\mathbf{u}^{k+1}$ using (24);
 $k := k + 1$;
until *convergence*;
 S_1: *Spectrum charging contract, on blockchain*
  Get final allocation scheme $\mathbf{z}^k$ from blockchain;
  Each MVNO pays for their allocated spectrum z_i^k .

Algorithm 2: Blockchain based distributed spectrum management scheme

---

IV. DYNAMIC SPECTRUM ALLOCATION AND POWER ALLOCATION DURING THE SECOND STAGE

During the second stage, each MVNO dynamically allocates the spectrum that has already been rent from MNO during the first stage to MUs in its serving region. The resource allocation can be performed during different time slots at the second stage and we only focus on a particular time slot. We further assume that perfect CSIs can be estimated by each MVNO at each time slot. Thus, the resource allocation optimization problem in the i-th MVNO can be formulated as

$$\min_{q_{ij}, b_{ij}} \sum_{j=1}^{N_i} q_{ij} \quad (25a)$$

$$\text{s.t.} \quad \sum_{j=1}^{N_i} b_{ij} \leq w_i \quad (25b)$$

$$b_{ij} \log_2\left(1 + \frac{q_{ij}|h_{ij}|^2}{b_{ij}n_0}\right) \geq \tilde{R}_i, \forall j \quad (25c)$$

$$q_{ij} \geq 0, b_{ij} \geq 0, \ \forall j, \quad (25d)$$

where $\tilde{R}_i$ denotes the QoS requirement of MUs in the i-th MVNO.

Lemma 1: For problem (25), the optimal variables q_{ij} and b_{ij} should satisfy that the QoS constraints in (25c) are all active, i.e.,

$$b_{ij} \log_2\left(1 + \frac{q_{ij}|h_{ij}|^2}{b_{ij}n_0}\right) = \tilde{R}_i, \forall j \quad (26)$$

Proof: We prove Lemma 1 by reductio ad absurdum. Assume that $q_{ij}^o, \forall j$ are the optimal solutions to (25) such that $b_{ij} \log_2\left(1 + \frac{q_{ij}^o|h_{ij}|^2}{b_{ij}n_0}\right) > \tilde{R}_i, \forall j$. Define a set of $\Delta q_{ij} > 0, \forall j$ such that

$$b_{ij} \log_2\left(1 + \frac{q_{ij}^o|h_{ij}|^2}{b_{ij}n_0}\right) > b_{ij} \log_2\left(1 + \frac{q_{ij}^\dagger|h_{ij}|^2}{b_{ij}n_0}\right), \forall j \quad (27)$$

where $q_{ij}^\dagger = q_{ij}^o - \Delta q_{ij}, \forall j$. Therefore, we can choose Δq_{ij} appropriately such that $b_{ij} \log_2\left(1 + \frac{q_{ij}^\dagger|h_{ij}|^2}{b_{ij}n_0}\right) = \tilde{R}_i, \forall j$. It is note that $q_{ij}^\dagger, \forall j$ are feasible and have smaller objective function value than $q_{ij}^o, \forall j$. ■

Combined with Lemma 1, problem (25) can be equivalently written as follows:

$$\min_{b_{ij}} \sum_{i=1}^{N_i} \frac{b_{ij}n_0}{|h_{ij}|^2}\left(2^{\frac{\tilde{R}_i}{b_{ij}}} - 1\right) \quad (28a)$$

$$\text{s.t.} \quad \sum_{j=1}^{N_i} b_{ij} \leq w_i \quad (28b)$$

$$b_{ij} \geq 0, \ \forall j. \quad (28c)$$

Problem (28) is convex and can be solved by convex optimization techniques. We can obtain the optimal spectrum allocation solution for (28) using the following proposition:

Proposition 2: The optimal spectrum allocation solution for (28), denoted by $b_{ij}^\star$, is

$$b_{ij}^\star = \frac{\hat{R}_i}{1 + \mathcal{W}_0\left(\frac{\mu^\star|h_{ij}|^2 - n_0}{en_0}\right)}, \forall j, \quad (29)$$

where $\hat{R}_i = \tilde{R}_i \ln 2$, $\mathcal{W}_0(\phi)$ is the branch satisfying $\mathcal{W}(\phi) \geq -1$ and $\mathcal{W}$ denotes the Lambert $\mathcal{W}$ function of ϕ [21], $\mu^\star > 0$ is a constant and can be obtained by using one-dimension (1-D) bisection search over interval $[\mu_{min}, \mu_{max}]$ with

$$\mu_{min} = \frac{n_0 e \left(\frac{N_i \hat{R}_i}{w_i} - 1 \right) e^{\left(\frac{N_i \hat{R}_i}{w_i} - 1 \right)} + n_0}{h_{max}} \tag{30}$$

$$\mu_{max} = \frac{n_0 e \left(\frac{N_i \hat{R}_i}{w_i} - 1 \right) e^{\left(\frac{N_i \hat{R}_i}{w_i} - 1 \right)} + n_0}{h_{min}} \tag{31}$$

where h_{max} and h_{min} denote the maximum and minimum channel gains among N_i users in the i-th MVNO, respectively.

Proof: See Appendix B. ∎

V. SIMULATION RESULTS

In this section, we evaluate the performance of our proposed spectrum leasing and allocation policies through numerical results.

We consider a multicell system consisting of six circular areas ($N = 6$) and each MVNO is located at the center of the cell. The radii and the corresponding user densities of the six cells are configured as ($r_1 = 80m, \lambda_1 = 2400/km^2$), ($r_2 = 80m, \lambda_2 = 1600/km^2$), ($r_3 = 100m, \lambda_3 = 1600/km^2$), ($r_4 = 100m, \lambda_4 = 2000/km^2$), ($r_5 = 120m, \lambda_5 = 2000/km^2$), and ($r_6 = 120m, \lambda_6 = 2400/km^2$). Each MVNO and corresponding MUs are equipped with one antenna. MUs are randomly and uniformly distributed within each cell. All the channels from MUs to corresponding MVNO are assumed to be subjected to three components: path-loss, log-normal shadowing, and small-scale Rayleigh fading. The path-loss decay factor is 3.76, path-loss at reference distance 1m is 15.3dB, the standard deviation for Shadowing is 8dB and Rayleigh small scale fading is 0dB. For (9), we set $K_i = 500, \forall i$. In all simulations, the total transmit power of each MVNO is computed by using 10000 randomly generated channel realizations. Noise spectral density of -174dBm/Hz and 10dBi antenna gain are considered. If not specified, the total bandwidth W_{sum} is set to be 100MHz and the minimum rate requirements R_{min} are set as $\bar{R}_i = \tilde{R}_i = R_{min} = 1Mbps, \forall i$.

In Fig. 2, we present the total transmit power P_{sum} comparison of different schemes for different path-loss decay factors α when the total bandwidth is 100MHz and the minimum rate requirement R_{min} is 1Mbps. Note that P_{sum} is defined as the total transmit power at the six MVNOs during the second stage. In the legend, "Proposed" denotes our proposed scheme where spectrum and power allocation factors are optimized during two stages. "DRA" denotes the dynamic resource allocation where the spectrum and power allocation factors are only optimized during the second stage and the spectrum is equally allocated during the first stage. "Reservation" denotes that the spectrum and power allocation factors are only optimized during the first stage and the spectrum is equally allocated during the second stage. "Benchmark" denotes the scheme that the spectrum is equally allocated both during the first stage and the second stage. It is observed that when the path-loss decay factor α increases, the total transmit power P_{sum} substantially increases for all
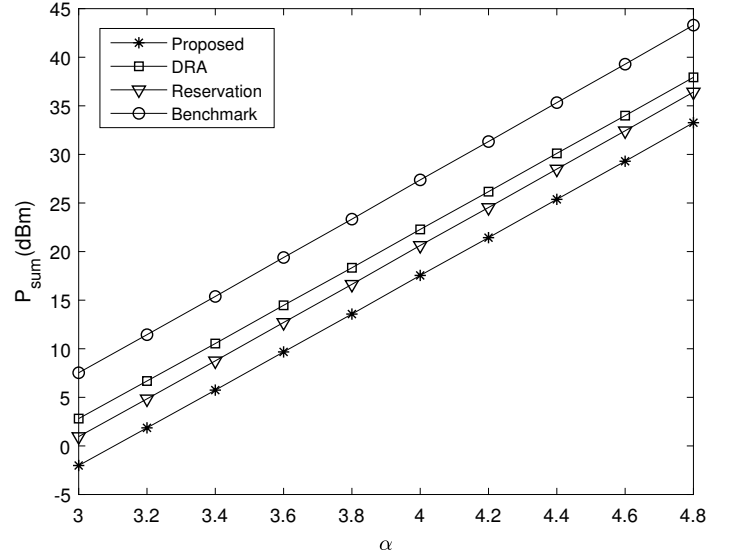

Fig. 2. Total transmit power P_{sum} at the six MVNOs versus the path-loss decay factor α; performance comparison of different schemes when the total bandwidth is 100MHz and the minimum rate requirement R_{min} is 1Mbps.
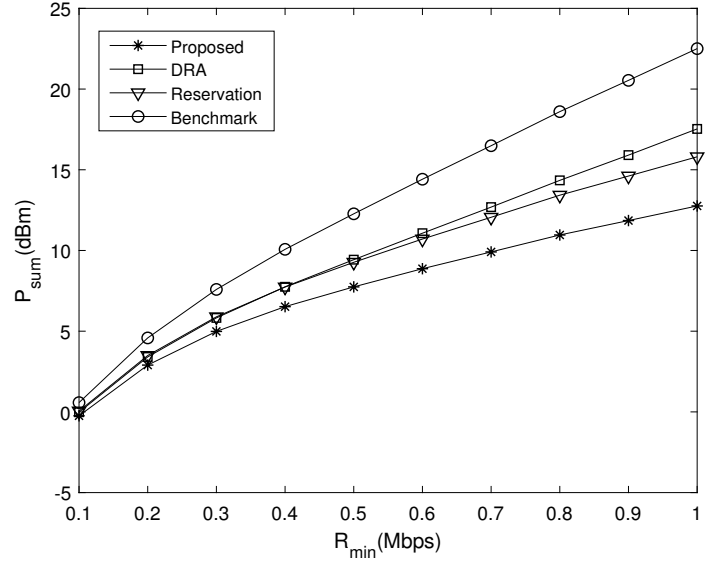

Fig. 3. Total transmit power P_{sum} at the six MVNOs versus the minimum rate requirement at MUs; performance comparison of different schemes when the total bandwidth is 100MHz and the path-loss decay factor is 3.76.

the schemes. Moreover, our proposed scheme is observed to achieve notably smaller total transmit power than the others schemes, which demonstrates the effectiveness of our proposed spectrum leasing and power allocation scheme.

In Fig. 3, we present the total transmit power P_{sum} comparison of different schemes for different minimum rate requirements R_{min} when the total bandwidth is 100MHz and the path-loss decay factor is 3.76. Here, we assume that $\bar{R}_i = \tilde{R}_i = R_{min}, \forall i$. From Fig. 3, it is observed that as the minimum rate requirement constraint R_{min} becomes more stringent, substantially more total transmit power P_{sum} is needed at the six MVNOs. In particular, the performance gap between our proposed scheme and the other schemes becomes larger when the minimum rate requirements R_{min} increases.
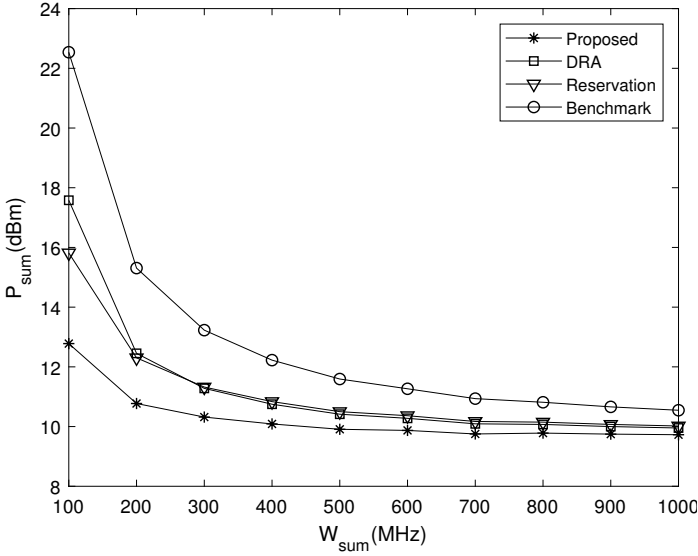
Fig. 4. Total transmit power P_{sum} at the six MVNOs versus the total bandwidth W_{sum} owned by the MNO; performance comparison of different schemes when the minimum rate requirement is 1Mbps and the path-loss decay factor is 3.76.

Fig. 6. Spectrum ratio versus the path-loss decay factor α when the minimum rate requirement is 1Mbps and the total bandwidth is 100MHz.
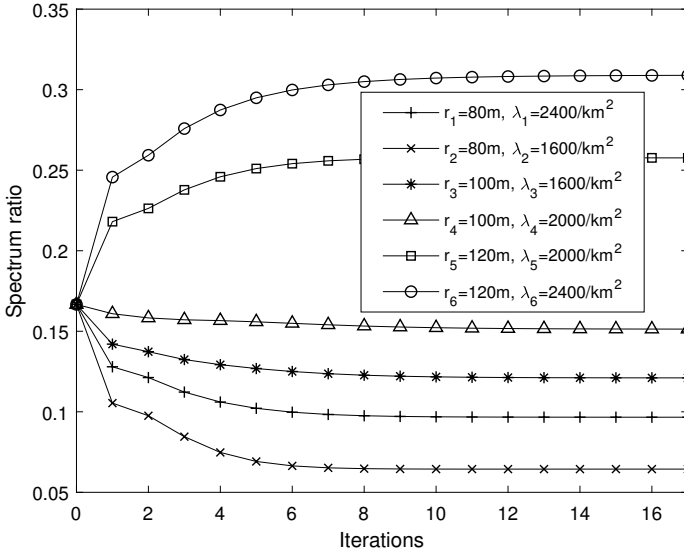

Fig. 5. Spectrum ratio versus the number of iterations at six MVNOs when the total bandwidth is 100MHz, the minimum rate requirement is 1Mbps, and the path-loss decay factor is 3.76.

In Fig. 4, we present the total transmit power P_{sum} comparison of different schemes for different total bandwidth W_{sum} when the minimum rate requirement is 1Mbps and the path-loss decay factor is 3.76. From Fig. 4, it is observed that as the total bandwidth W_{sum} increases, the total transmit power P_{sum} substantially decreases for all schemes. It is also found that our proposed scheme outperforms the other schemes.

In Fig. 5, we present the spectrum ratio occupied by each MVNO for different iteration times when the total bandwidth is 100MHz and the minimum rate requirement is 1Mbps, where spectrum ratio is defined as the ratio of the bandwidth occupied by the MVNO to the total bandwidth. It is found from Fig. 2 that after only 6~8 iterations, the steady spectrum
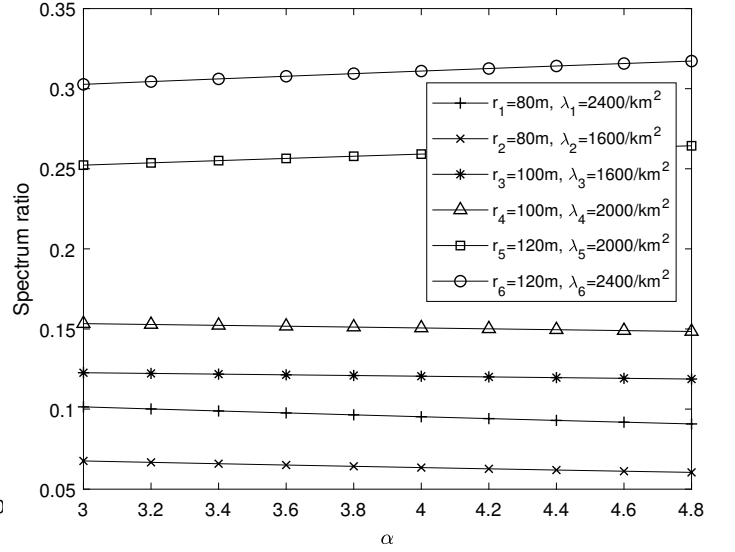
ratio is achieved. It is also found that both radius and user density in the MVNO have significant effects on the spectrum ratio. The larger the radius of the cell is configured, the more bandwidth is needed. Likewise, the larger the user density of the cell is configured, the more bandwidth is needed. The main reason behind this phenomenon is that when the user densities of different cells are the same, the channel conditions in cells with large radius are poorer than those with small radius. Thus, more spectrum is needed in large cells for satisfying the QoS of the MUs with poor channel conditions to reduce the total transmit power. Similarly, when the radii of different cells are the same, more spectrum is needed in cells with large user densities than whose with small user densities to meet the QoS constraints.

In Fig. 6, we present the spectrum ratio occupied by each MVNO for different path-loss decay factors, α, when the total bandwidth is 100MHz and the minimum rate requirement is 1Mbps. For simplicity, the MVNO with above-average spectrum value is denoted as "LMVNO" and the MVNO with below-average spectrum value is denoted as "SMVNO". From Fig. 6, it is observed that the MNO allocates more spectrum to LMVNOs and less spectrum to SMVNOs as α increases. This is because the number of MUs in LMVNOs with poor channel conditions is larger than in SMVNOs and those MUs in LMVNOs with poor channel conditions are more sensitive to the path-loss decay factor α. Consequently, more spectrum is needed in LMVNOs to reduce the total transmit power.

In Fig. 7, we present the spectrum ratio for different total bandwidths W_{sum} owned by the MNO when the minimum rate requirement is 1Mbps and the path-loss decay factor is 3.76. The results in Fig. 7 show that more spectrum is allocated to SMVNO and less spectrum is allocated to LMVNO as W_{sum} decreases. The reason behind this phenomenon is that from (26), we can observe that the power allocation factor monotonically decreases as the bandwidth increases. Thus, when the bandwidth is in shortage, if we decrease the spectrum
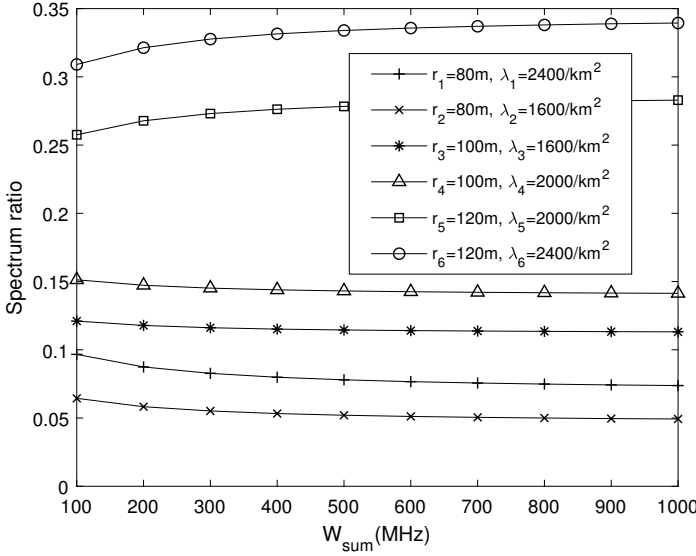
Fig. 7. Spectrum ratio versus the total bandwidth W_{sum} owned by the MNO when the minimum rate requirement is 1Mbps and the path-loss decay factor is 3.76.
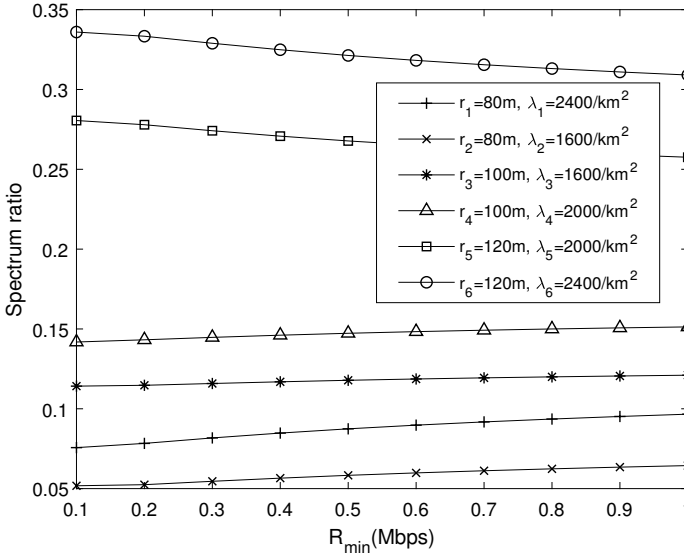

Fig. 8. Spectrum ratio versus the minimum rate requirements at six MVNOs when the total bandwidth is 100MHz and the path-loss decay factor is 3.76.

allocated to the MUs in SVMNOs, the total transmit power will increase drastically. Consequently, in order to minimize the total transmit power, more spectrum should be allocated to the MUs in SVMNOs when W_{sum} decreases.

In Fig. 8, we present the spectrum ratio for different minimum rate requirements when the total bandwidth is 100MHz and the path-loss decay factor is 3.76. From Fig. 8, it is observed that more spectrum is allocated to SMVNO and less spectrum is allocated to LMVNO as R_{min} increases. This is because the transmission rate is monotonically increasing with respect to the bandwidth (26), which means that the bandwidths are more needed when the QoS constraints get more stringent. This coincides with situation that the spectrum is in shortage and thus more spectrum should be allocated to the MUs in SVMNOs when R_{min} increases.

VI. CONCLUSION

APPENDIX A
PROOF OF PROPOSITION 1

The CDF of $|h_{ij}|^2$ is calculated as follows:

$$
\begin{aligned}
F_{|h_{ij}|^2}(x) &= Prob\left(\frac{|g_{ij}|^2}{1+d_{ij}^\alpha} \leq x\right) \\
&= Prob\left(|g_{ij}|^2 \leq x\left(1+d_{ij}^\alpha\right)\right) \\
&\overset{(a)}{=} \int_{\mathcal{D}(o_i,r_i)} \frac{1}{\pi r_i^2}\left(1-e^{-x\left(1+d_{ij}^\alpha\right)}\right)d\Delta S \\
&\overset{(b)}{=} \frac{1}{\pi r_i^2}\int_0^{r_i}\int_{-\pi}^{\pi}\left(1-e^{-x(1+y^\alpha)}\right)yd\theta dy \\
&= \frac{2}{r_i^2}\int_0^{r_i}\left(y-ye^{-x(1+y^\alpha)}\right)dy \\
&= \frac{2}{r_i^2}\int_0^{r_i}ydy - \frac{2}{r_i^2}\int_0^{r_i}ye^{-x(1+y^\alpha)}dy \\
&= 1 - \frac{2}{r_i^2}e^{-x}\int_0^{r_i}ye^{-xy^\alpha}dy
\end{aligned}
\tag{32}
$$

where (a) follows from the CDF of the exponential random variable $|g_{ij}|^2$, (b) follows by using polar coordinates. Let $t = xy^\alpha$, $F_{|h_{ij}|^2}(x)$ can be further derived as follows:

$$
\begin{aligned}
F_{|h_{ij}|^2}(x) &= 1 - \frac{2}{r_i^2}e^{-x}\int_0^{xr_i^\alpha}t^{\frac{1}{\alpha}}x^{-\frac{1}{\alpha}}e^{-t}d\left(t^{\frac{1}{\alpha}}x^{-\frac{1}{\alpha}}\right) \\
&= 1 - \frac{1}{\alpha}\frac{2}{r_i^2}x^{-\frac{2}{\alpha}}e^{-x}\int_0^{xr_i^\alpha}t^{\frac{2}{\alpha}-1}e^{-t}dt \\
&= 1 - \frac{2}{\alpha}(xr_i^\alpha)^{-\frac{2}{\alpha}}\gamma\left(\frac{2}{\alpha},xr_i^\alpha\right)e^{-x} \\
&\overset{(c)}{=} 1 - M\left(\frac{2}{\alpha},1+\frac{2}{\alpha},-xr_i^\alpha\right)e^{-x}
\end{aligned}
\tag{33}
$$

where $\gamma(s,x) = \int_0^x t^{s-1}e^{-t}dt$ denotes the lower incomplete gamma function, $M(a,b,z)$ denotes the Kummer's function [13], (c) follows from $\gamma(s,x) = s^{-1}x^s M(s,s+1,-x)$. Thus the proof is completed.

APPENDIX B
PROOF OF PROPOSITION 2

The Lagrangian of problem (28) is given by

$$
\begin{aligned}
\mathcal{L}(b_{ij},\mu) &= \sum_{i=1}^{N_i}\frac{b_{ij}n_0}{|h_{ij}|^2}\left(2^{\frac{\tilde{R}_i}{b_{ij}}}-1\right) + \mu\left(\sum_{j=1}^{N_i}b_{ij}-w_i\right) \\
&\overset{(h)}{=} \sum_{i=1}^{N_i}\frac{b_{ij}N_0}{|h_{ij}|^2}\left(e^{\frac{\hat{R}_i}{b_{ij}}}-1\right) + \mu\left(\sum_{j=1}^{N_i}b_{ij}-w_i\right)
\end{aligned}
\tag{34}
$$

where $\mu \geq 0$ denotes the Lagrange multiplier associated with the constraint (28b). (h) follows from $\hat{R}_i = \tilde{R}_i\ln 2$. Thus, the dual function of problem (28) is given by

$$
\mathcal{G}(\mu) = \min_{b_{ij}\geq 0}\mathcal{L}(b_{ij},\mu)
\tag{35}
$$

It can be seen from problem (28) that there exist a set of b_{ij} with $b_{ij} \geq 0$, satisfying $\sum_{j=1}^{N_i} b_{ij} \leq w_i, \forall j$. Thus, thanks to the Slater's condition, strong duality for problem (28) holds. The Karush-Kuhn-Tucker (KKT) conditions which are both necessary and sufficient for the global optimality of problem (28) are given by

$$\frac{\partial \mathcal{L}\left(b_{ij}^{\star}, \mu^{\star}\right)}{\partial b_{ij}} = 0 \tag{36}$$

$$\mu^{\star} \left(\sum_{j=1}^{N_i} b_{ij}^{\star} - w_i\right) = 0 \tag{37}$$

$$\sum_{j=1}^{N_i} b_{ij}^{\star} - w_i \leq 0 \tag{38}$$

where $b_{ij}^{\star}$ and $\mu^{\star}$ denote the optimal primal and dual solutions of problem (28), respectively. It can be easily verified that $\sum_{j=1}^{N_i} b_{ij}^{\star} = w_i$ must hold for problem (28). Thus, from (37), we have $\mu^{\star} > 0$. From (36), it follows that

$$\begin{aligned}
\frac{\partial \mathcal{L}\left(b_{ij}^{\star}, \mu^{\star}\right)}{\partial b_{ij}} &= \frac{n_0}{|h_{ij}|^2} \left(e^{\frac{\hat{R}}{b_{ij}^{\star}}} - \frac{\hat{R}_i}{b_{ij}^{\star}} e^{\frac{\hat{R}_i}{b_{ij}^{\star}}} - 1\right) + \mu^{\star} \\
&= \frac{n_0}{|h_{ij}|^2} \left(\left(1 - \frac{\hat{R}_i}{b_{ij}^{\star}}\right) e^{\frac{\hat{R}_i}{b_{ij}^{\star}} - 1} e - 1\right) + \mu^{\star} \\
&= 0.
\end{aligned} \tag{39}$$

From (39), we have

$$\left(\frac{\hat{R}_i}{b_{ij}^{\star}} - 1\right) e^{\frac{\hat{R}}{b_{ij}^{\star}} - 1} = \frac{\mu^{\star} |h_{ij}|^2 - n_0}{n_0 e}, \tag{40}$$

according to the definition of Lambert $\mathcal{W}$ function, we can obtain the optimal $W_{ij}^{\star}$ as follows:

$$b_{ij}^{\star} = \frac{\hat{R}_i}{1 + \mathcal{W}_0 \left(\frac{\mu^{\star} |h_{ij}|^2 - n_0}{n_0 e}\right)}, \tag{41}$$

where $\mathcal{W}_0(\phi)$ is the branch satisfying $\mathcal{W}(\phi) \geq -1$, $\mathcal{W}$ denotes the Lambert $\mathcal{W}$ function of ϕ [21] and the optimal $\mu^{\star}$ can be obtained via a 1-D bisection search over $[\mu_{min}, \mu_{max}]$ with μ_{min} and μ_{max} derived as follows.

Denote the maximum and minimum channel gains among N_i users in the i-th MVNO as h_{max} and h_{min}, respectively. Thus, we have

$$h_{min} \leq |h_{ij}|^2 \leq h_{max}. \tag{42}$$

Since $\mathcal{W}(x)$ is monotonically increasing when $x \geq 0$, it follows that

$$\begin{aligned}
&\mathcal{W}_0 \left(\frac{\mu^{\star} h_{min} - n_0}{n_0 e}\right) \\
&\leq \mathcal{W}_0 \left(\frac{\mu^{\star} |h_{ij}|^2 - n_0}{n_0 e}\right) \leq \mathcal{W}_0 \left(\frac{\mu^{\star} h_{max} - n_0}{n_0 e}\right)
\end{aligned} \tag{43}$$

Combined with (41), the above inequality can be reformulated as

$$\frac{\hat{R}_i}{1 + \mathcal{W}_0 \left(\frac{\mu^{\star} h_{max} - n_0}{n_0 e}\right)} \leq b_{ij}^{\star} \leq \frac{\hat{R}_i}{1 + \mathcal{W}_0 \left(\frac{\mu^{\star} h_{min} - n_0}{n_0 e}\right)} \tag{44}$$

After adding each term in (44) from $j = 1$ to $j = N_i$, we can obtain the following inequality

$$\frac{N_i \hat{R}_i}{1 + \mathcal{W}_0 \left(\frac{\mu^{\star} h_{max} - n_0}{n_0 e}\right)} \leq w_i \leq \frac{N_i \hat{R}_i}{1 + \mathcal{W}_0 \left(\frac{\mu^{\star} h_{min} - n_0}{n_0 e}\right)} \tag{45}$$

Finally, we have

$$\mu_{min} \leq \mu^{\star} \leq \mu_{max} \tag{46}$$

where

$$\mu_{min} = \frac{n_0 e \left(\frac{N_i \hat{R}_i}{w_i} - 1\right) e^{\left(\frac{N_i \hat{R}_i}{w_i} - 1\right)} + n_0}{h_{max}} \tag{47}$$

$$\mu_{max} = \frac{n_0 e \left(\frac{N_i \hat{R}_i}{w_i} - 1\right) e^{\left(\frac{N_i \hat{R}_i}{w_i} - 1\right)} + n_0}{h_{min}} \tag{48}$$

The proof is completed.

REFERENCES

[1] N. Panwar, S. Sharma, and A. K. Singh, "A survey on 5G: The next generation of mobile communication," *Phys. Commun.*, vol. 18, pp. 64-84, Mar. 2016.

[2] N. Al-Falahy and O. Y. Alani, "Technologies for 5G networks: Challenges and opportunities," *IT Prof.*, vol. 19, no. 1, pp. 12-20, Jan./Feb. 2017.

[3] C. Liang and F. R. Yu, "Wireless network virtualization: A survey, some research issues and challenges, *IEEE Comm. Surveys Tutorials*, vol. 17, pp. 358380, Firstquarter 2015.

[4] R. Kokku, R. Mahindra, H. Zhang, and S. Rangarajan, "Nvs: A substrate for virtualizing wireless resources in cellular networks," *IEEE/ACM Trans. Netw.*, vol. 20, no. 5, pp. 13331346, Oct. 2012

[5] L. Zhao, M. Li, Y. Zaki, A. Timm-Giel and C. Gorg, "LTE virtualization: From theoretical gain to practical solution," *in Proc. International Teletraffic Congress (ITC)*, pp. 7178, Sep. 2011.

[6] 3GPP TR 22.852, "Study on Radio Access Network (RAN) sharing enhancements," Jun. 2013.

[7] X. Costa-Perez, J. Swetina, T. Guo, R. Mahindra, and S. Rangarajan, "Radio access network virtualization for future mobile carrier networks," *IEEE Commun. Mag.*, vol. 51, no. 7, pp. 27-35, Jul. 2013.

[8] M. I. Kamel, L. Bao Le, and A. Girard, "LTE wireless network virtualization: dynamic slicing via flexible scheduling," *in Proc. IEEE VTC Fall*, pp. 1-5, Sept. 2014.

[9] M. Kalil, A. Moubayed, A. Shami, and A. Al-Dweik, "Efficient low-complexity scheduler for wireless resource virtualization," *IEEE Wireless Commun. Letters*, vol. 5, no. 1, pp. 56-59, Feb 2016.

[10] Y. Zhang, S. Bi, and Y. J. A. Zhang, "A two-stage spectrum leasing optimization framework for virtual mobile network operators," in *IEEE Int. Conf. on Commun. Syst. (ICCS)*, Dec. 2016, pp. 16.

[11] Y. Zhang, S. Bi, and Y.-J. A. Zhanga, "Joint Spectrum Reservation and On-demand Request for Mobile Virtual Network Operators," *IEEE Trans. Commun.*, vol. 66, no. 7, pp. 2966-2977, July, 2018.

[12] J. G. D. Forney and G. Ungerboeck, "Modulation and coding for linear gaussian channels," *IEEE Trans. Inf. Theory*, vol. 44, no. 6, Oct. 1998.

[13] M. Abramowitz and I. A. Stegun, Handbook of mathematical functions: with formulas, graphs, and mathematical tables, vol. 55. *Courier Corporation*, 1965.

[14] J. S. Ball, "Half-range generalized Hermite polynomials and the related Gaussian quadratures," *SIAM J. Numer. Anal.*, vol. 40, no. 6, pp. 2311-2317, 2002.

[15] N. M. Steen, G. D. Byrne, and E. M. Gelbard, "Gaussian quadratures for the integrals $\int_0^{\infty} e^{-x^2} f(x)\, dx$ and $\int_0^b e^{-x^2} f(x)\, dx$," *Math. Comput.*, vol. 23, no. 107, pp. 661-671, 1969.

[16] M. Grant and S. Boyd, *CVX: MATLAB Software for Disciplined Convex Programming.* Version 2.1, 2016, available: http://cvxr.com/cvx.

[17] S. Boyd, N. Parikh, E. Chu, B. Peleato, and J. Eckstein, "Distributed optimization and statistical learning via the alternating direction method of multipliers," *Found. Trends in Mach. Learn.*, vol. 3, no. 1, pp. 1122, Jan. 2011.

[18] E. Chen and M. Tao, "ADMM-based fast algorithm for multi-group multicast beamforming in large-scale wireless systems," *IEEE Trans. Commun.*, vol. 65, no. 6, pp. 26852698, Jun. 2017.

[19] S. Boyd and L. Vandenberghe, Convex Optimization. Cambridge, U.K.: Cambridge Univ. Press, 2004.

[20] J. Duchi, S.Shalev-Shwartz, Y. Singer, and T. Chandra, "Efficient projections onto the l_1-ball for learning in high dimensions," in *Proc. 25th Int. Conf*. Mach. Learn., 2008, DOI: 10.1145/1390156.1390191.

[21] R. M. Corless, G. H. Gonnet, D. E. G. Hare, D. J. Jeffrey, and D. E. Knuth, "On the Lambert W function," *Adv. Comput. Math.*, vol. 5, pp. 329-359, 1996.